Talanta 134 (2015) 754–760

Contents lists available at ScienceDirect

Talanta

journal homepage: www.elsevier.com/locate/talanta

Effects of (R)- and (S)-propranolol hydrochloride enantiomers on the resonance Rayleigh scattering spectra with erythrosine B as probe and their analytical applications

Jidong Yang [a,b,c,*], Ernv Wang [a], Shang Zhou [b], Qiong Yang [b]

[a] School of Chemistry and Chemical Engineering, Southwest University, Chongqing 400715, P. R. China
[b] School of Chemistry and Chemical Engineering, Yangtze Normal University, Fuling, Chongqing 408100, P. R. China
[c] School of Chemistry and Environment Engineering, Chongqing Three Gorges University, Wanzhou, Chongqing 404100, P. R. China

ARTICLE INFO

Article history:
Received 20 August 2014
Received in revised form
19 December 2014
Accepted 20 December 2014
Available online 30 December 2014

Keywords:
Resonance Rayleigh scattering
(S)-propranolol hydrochloride
(R)-propranolol hydrochloride
Erythrosine B

ABSTRACT

Propranolol, a chiral drug with two configurations, i.e., (R)-propranolol hydrochloride (RPH) and (S)-propranolol hydrochloride (SPH), has racemes that can be used in clinical diagnosis due to their synergistic effects. SPH has a β-receptor blocking effect, and RPH has an antiarrhythmic effect. In pH 4.6 Britton-Robinson (BR) buffer solution, both RPH and SPH can react with erythrosine B to form 1:1 ion-association complexes. In the SPH-Ery B reaction system, a remarkable enhancement of the resonance Rayleigh scattering (RRS) signal located at 338 nm was observed. However, a similar phenomenon was not obvious and was unstable in the RPH-Ery B reaction system. Based on this result, a simple, novel and sensitive method for the determination of SPH was proposed based on the RRS technique. The linear range and limit of detection were 0.0680～4.0 μg mL^{-1} and 20.6 ng mL^{-1}, respectively. Additionally, the spectroscopic approaches of frequency doubling scattering (FDS) and second-order scattering (SOS) were also proposed for SPH detection in this article. The interaction information regarding the mechanism of the reaction, suitable reaction conditions, influencing factors and the effects of mixed solutions were our investigation aims. The method had been applied to the determination of SPH in fresh serum and urine samples of healthy human subjects with satisfactory results.

1. Introduction

(R)-, (S)-propranolol hydrochloride (i.e., RPH and SPH), known as propranlolum, are important chiral, racemic drugs that have been used to treat heart disease in clinical practice. The synergistic effect of SPH is approximately 100 times greater than that of RPH when it is used as a β-receptor blocking drug, whereas RPH has a stronger antiarrhythmic and membrane stabilizing effect. Therefore, the chiral drug is an effective enantiomer; its combined pharmacological effect is greater than any single enantiomer [1,2]. Based on this behavior, it is necessary to explore the chiral recognition and different pharmacodynamics of enantiomer drugs for more effective and scientific clinical application. At present, few spectrophotometric methods for chiral recognition have been reported, but there have been a few methods for the determination of propranolol hydrochloride, such as capillary electrophoresis [1], spectrophotometry [3–5], fluorescence spectrometry [6], charge-transfer reaction [7], high-performance liquid chromatography (HPLC) [8], and flow injection chemiluminescence [9]. Among these methods, HPLC is widely used for the determination of propranolol hydrochloride because of its high sensitivity. However, HPLC requires some complex pretreatments and cannot be directly used for the simultaneous determination of enantiomers. Therefore, it is crucial to develop a sensitive, simple, selective and rapid method for the direct simultaneous determination of trace (R)-,(S)-chiral drugs without separating them in advance.

Resonance Rayleigh scattering (RRS) is a special elastic scattering, and it also has a special synchronous fluorescence of $\Delta\lambda=0$ (i.e., $\lambda_{em}=\lambda_{ex}$), which occurs when the wavelength of the Rayleigh scattering spectral band is located at or close to the molecular absorption band. Second-order scattering and frequency doubling scattering are resonance nonlinear scattering (RNLS). When incident light with shorter wavelengths passes through a sample, second order scattering (SOS) appears at $\lambda_{em}=2\lambda_{ex}$. When incident light with longer wavelengths passes through a sample, frequency doubling scattering (FDS) appears at $\lambda_{em}=1/2\lambda_{ex}$. Because of their high sensitivity, simplicity and better selectivity, RRS and RNLS have proven to be important analytical methods for the determination of biological macromolecules, such as nucleic acids [10], proteins [11], polysaccharides, including hyaluronic acid

* Corresponding author at: School of Chemistry and Environment Engineering, Chongqing Three Gorges University, Wanzhou, Chongqing 404100, P. R. China. Tel.: +86 18996678896.
E-mail address: sxyjd7600@sina.com (J. Yang).

http://dx.doi.org/10.1016/j.talanta.2014.12.030
0039-9140/

[12], dextran sulfate sodium [13], chondroitin sulfate A [14], heparin [15], etc. Additionally, they have been used to determine inorganic ions [16,17], organic compounds [18,19], and pharmaceuticals [20–22]. However, there have been no reports of the direct, simultaneous determination of chiral drugs using RRS or RNLS. In this article, a highly sensitive analytical method for chiral recognition in enantiomer drugs has been developed based on the RRS technique.

In this study, the interactions of some halofluorescein dyes, such as eosin Y, erythrosine, rose bengal and erythrosine B, with (R)-, (S)-propranolol hydrochloride were investigated. The corresponding results indicated that erythrosine B was the best probe reagent for the determination of (S)-propranolol hydrochloride. In a pH 4.6 Britton-Robinson (BR) buffer solution, the chiral drug existed as a univalent cation, and erythrosine B existed as a univalent anion, which resulted in the formation of a 1:1 ion-association complex and a change in their absorption spectra due to the electrostatic interaction. A new RRS spectrum appeared in the SPH-Ery B system, but the RRS spectrum was very weak and unstable. In addition, the intensities of the RRS, FDS and SOS in the SPH-Ery B system were significantly enhanced, and the intensity of the RRS was much greater than that of the SOS, FDS and absorption spectra. Therefore, the RRS method was used as an example for the following studies: the optimum conditions, effects of coexisting substances and analytical applications. The mechanism of ion-association and the reasons for the RRS enhancement were also studied using spectroscopic approaches and quantum chemical calculations. Based on the above primary analysis, a sensitive, simple, selective and rapid method using Ery B as an RRS probe for the trace determination of (S)-propranolol hydrochloride in serum and urine samples was proposed in this article for the first time.

2. Experimentation

2.1. Apparatus

A Hitachi F-2500 fluorospectrophotometer (Hitachi Company, Tokyo, Japan) was used to measure the scattering intensities with slits (EX/EM) of 5.0/5.0 nm (RRS, SOS and FDS). A UV-4100 UV/VIS/NIR spectrophotometer (Hitachi Company, Tokyo, Japan) was used to record the absorption spectra. A pH-S20K meter (Mettler-Toledo Instruments Co., Shanghai, China) was used to adjust the pH values of the aqueous solutions.

2.2. Reagents

A working solution of erythrosine B (Ery B, Tianjin Chemical Reagent Factory, China) 3.6×10^{-4} mol·L^{-1} was prepared. The standard solutions of (S)-propranolol hydrochloride (SPH) and (R)-propranolol hydrochloride (RPH) were prepared at concentrations of 100 μg mL^{-1} by weighing and dissolving in doubly distilled water, and then further diluted with water to 20 μg mL^{-1} for use as working solutions. Britton-Robinson (BR) buffer solutions with different pH were prepared by mixing 0.2 mol L^{-1} NaOH with a mixture of 0.04 mol L^{-1} H_3PO_4, H_3BO_3 and HAc in different proportions. All reagents were of analytical grade and used without further purification. The water used throughout was doubly distilled.

2.3. Procedure

First, 2.0 mL of pH 4.6 BR buffer solution, suitable amounts of SPH or RPH solution and 1.0 mL Ery B solution were added to a 10-mL calibrated flask. Then, this mixture was diluted to the calibration mark with water and thoroughly mixed. After 10 min, RRS spectra of the system were recorded using synchronous scanning at $\lambda_{em}=\lambda_{ex}$, and SOS and FDS spectra were recorded by scanning at $\lambda_{em}=2\lambda_{ex}$ and $\lambda_{em}=1/2\lambda_{ex}$, respectively. Then, the scattering intensities, I_{RRS}, I_{SOS} and I_{FDS} for the reaction product and I°_{RRS}, I^{0}_{SOS} and I^{0}_{FDS} for the reagent blank, were measured at their maximum wavelengths: $\Delta I_{RRS}=I_{RRS}-I^{0}_{RRS}$, $\Delta I_{SOS}=I_{SOS}-I^{0}_{SOS}$ and $\Delta I_{FDS}=I_{FDS}-I^{0}_{FDS}$. The absorption spectra and fluorescence spectra were recorded simultaneously.

3. Results and discussion

3.1. RRS spectra

RRS spectra of the SPH/RPH-Ery B system are shown in Fig. 1. The RRS intensities of single SPH, RPH and Ery B were very weak (Fig. 1a). While new RRS spectra appeared when SPH and RPH reacted with Ery B, the RRS intensities were both remarkably enhanced. A more interesting phenomenon is that the RRS intensity of the SPH-Ery B system was higher than that of RPH-Ery B system, and the latter was very unstable. The maximum and secondary RRS wavelengths of SPH-Ery B were located at 369 nm and 338 nm, respectively, and a new weaker peak appeared at 578 nm. Fig. 1b indicated that the enhancement of the RRS intensity at 338 nm was directly proportional to the concentration of SPH with a better

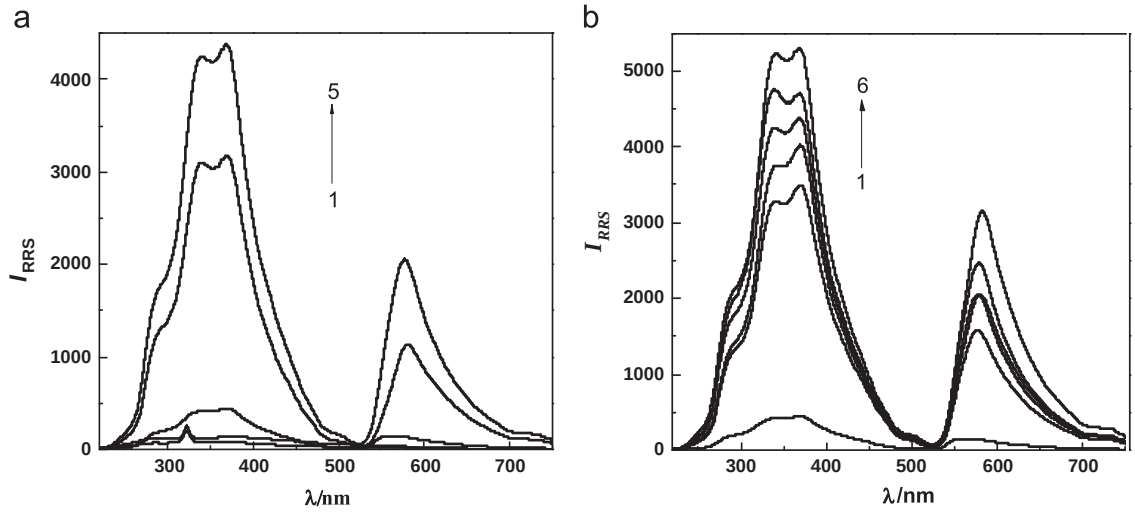

Fig. 1. RRS spectra of SPH-EryB system (a) 1. SPH; 2. RPH; 3. EryB; 4. RPH-EryB; 5. SPH-EryB. C_{RPH}: 2.4 μg mL^{-1}; C_{SPH}: 2.4 μg mL^{-1}; $C_{Ery\ B}$: 3.6×10^{-5} mol L^{-1}; BR, pH=4.6. (b) SPH-Ery B system. C_{SPH} (1–6): 0, 0.8, 1.6, 2.4, 3.2, 4.0 μg mL^{-1}; $C_{Ery\ B}$: 3.6×10^{-5} mol L^{-1}; BR,pH=4.6.

linear relationship for SPH detection. Therefore, the RRS method can be applied for the quantitative determination of trace SPH.

3.2. SOS spectra and FDS spectra

As shown in Fig. 2 and Fig. 3, the SOS and FDS spectra of the SPH-Ery B system were revealed. However, the corresponding SOS and FDS spectra of the RPH-Ery B system were not demonstrated because of their weakness and instability. It was found that the initial SOS and FDS intensities of SPH and Ery B were very weak, as shown in Fig. 2a and Fig. 3a, whereas the SOS and FDS intensities of Ery B were dramatically enhanced in the presence of SPH; new spectral characteristics of SOS and FDS appeared under the experimental conditions. These phenomena further demonstrated the formation of ion-association complexes between SPH and Ery B. The maximum wavelength ($\lambda_{ex}/\lambda_{em}$) of SOS was located at 320 nm/640 nm, and the maximum wavelength ($\lambda_{ex}/\lambda_{em}$) of FDS was located at 780 nm/390 nm. In addition, there were also a SOS peaks at 290 nm/580 nm, but the intensity of the reagent blank was relatively larger. Due to the high signal-to-noise ratio, 320 nm/640 nm and 780 nm/390 nm were selected as the detection wavelengths [23]. As shown in Fig. 2b and Fig. 3b, it is very obvious that the enhancement of the SOS and FDS intensities in the SPH-Ery B system were directly proportional to the concentration of SPH over a certain range. According to the above primary analysis, the SOS and FDS approaches can be applied to the monitoring of SPH as well.

3.3. Absorption spectra and fluorescence spectra

UV–vis absorption spectra measurement is a very simple method that is applicable to the determination of complex formation and the exploration of structural change. To measure the reaction of Ery B with SPH and RPH, absorption spectra of the SPH-Ery B system and the RPH-Ery B system were obtained. As shown in Fig. 4, it was not hard to determine that the absorptions of SPH and RPH in regions of near visible light were relatively weak, while there is a strong absorption by Ery B with a maximum absorption peak located at 522 nm. When Ery B reacted with SPH or

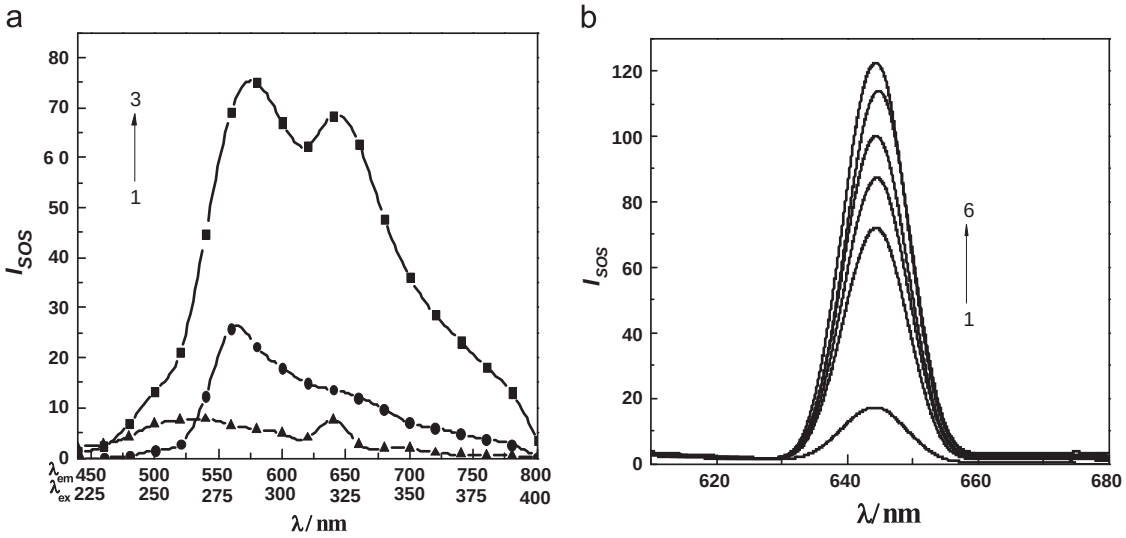

Fig. 2. SOS spectra of SPH-EryB system (a) 1. SPH; 2. Ery B; 3. SPH-Ery B; C_{SPH}: 2.4 μg mL^{-1}; C_{EryB}: 3.6×10^{-5} mol L^{-1} (b) SPH-Ery B system. C_{SPH} (1–6) 0, 0.8, 1.6, 2.4, 3.2, 4.0 μg mL^{-1}; $C_{Ery\ B}$: 3.6×10^{-5} mol L^{-1}; BR, pH=4.6.

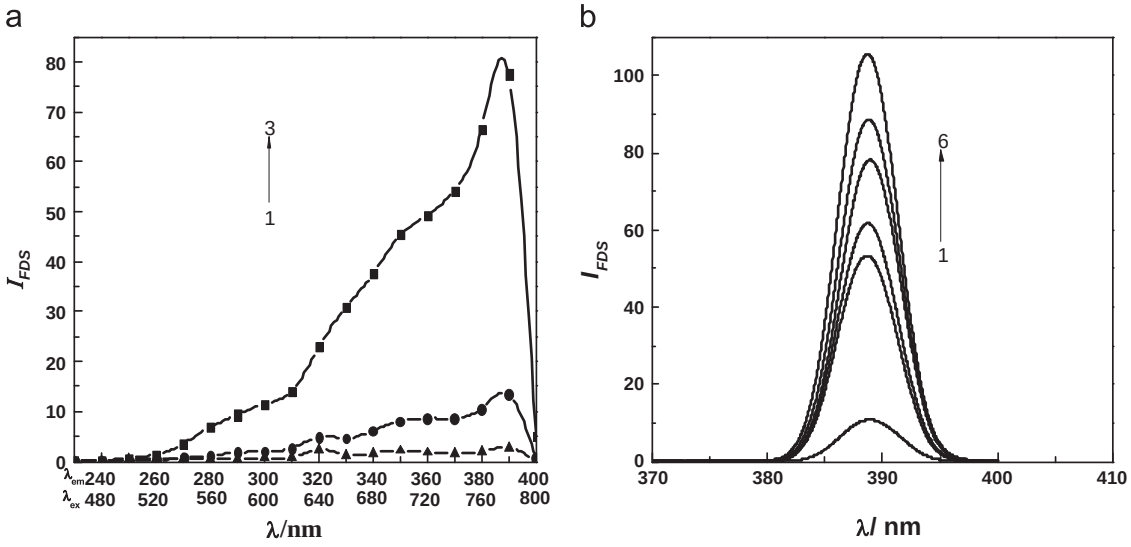

Fig. 3. FDS spectra of SPH-Ery B system (a) 1. SPH; 2. Ery B; 3. SPH-Ery B; C_{SPH}: 2.4 μg mL^{-1}, $C_{Ery\ B}$: 3.6×10^{-5} mol × L^{-1} (b) SPH-Ery B system. C_{SPH} (1–6): 0, 0.8, 1.6, 2.4, 3.2, 4.0 μg mL^{-1}; $C_{Ery\ B}$: 3.6×10^{-5} mol L^{-1}; BR, pH=4.6.

RPH to form ion-association complexes, its maximum absorption at 522 nm decreased, and the absorption intensity was directly proportional to the concentration of SPH or RPH. The fluorescence peaks of SPH and RHP were all located at Ex/Em=291 nm/339 nm, while that of Ery B was located at Ex/Em=538 nm/557 nm, and the intensity of Ery B was lower than that of SPH and RHP. When RPH and SPH reacted with Ery B to form ion-association complexes, the RPH and SPH fluorescences were quenched by RPH-Ery B and SPH-Ery B at the wave site of RPH and SPH, while the Ery B fluorescence was quenched by RPH-Ery B and SPH-Ery B at the wave site of Ery B.

3.4. Optimum reaction conditions

3.4.1. Effect of acidity

The influences of different types of buffer solutions, including BR, HAc-NaAc, and Na_2HPO_4-citrate, on the RRS intensity were tested. The results showed that BR was better than the other buffer solutions with an optimum pH range of 4.5～4.7. When the pH was lower than 4.5 or higher than 4.7, the ΔI intensity of the system decreased significantly (Fig. 5). Therefore, pH 4.6 was chosen as the reaction acidity, and 2.0 mL was specified as the appropriate volume of buffer solution.

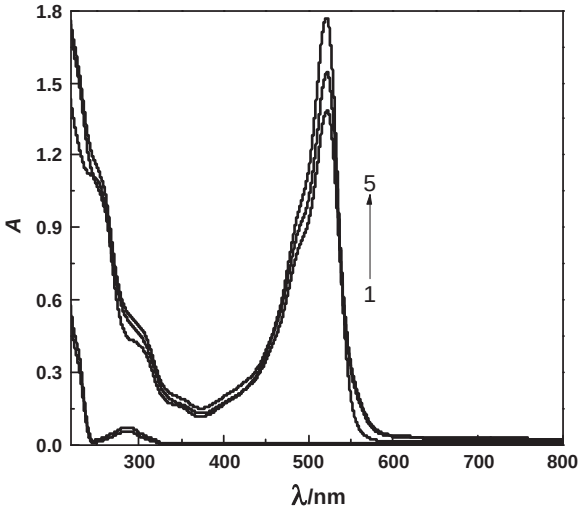

Fig. 4. Absorption spectra Measured against reagent blank. 1. RPH; 2. SPH; 3. SPH-EryB; 4. RPH-Ery B; 5. Ery B; C_{SPH}: 2.4 μg mL^{-1}; $C_{Ery\ B}$: 3.6×10^{-5} mol L^{-1}; BR, pH=4.6.

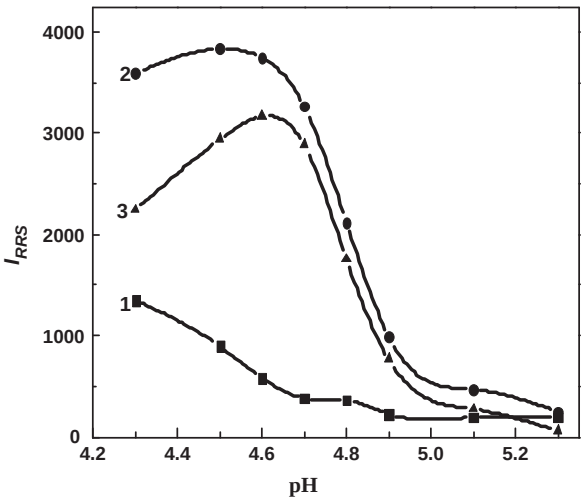

Fig. 5. Effect of acidity 1. I^0; 2. I; 3. ΔI, $C_{Ery\ B}$: 3.6×10^{-5} mol Ll^{-1}; C_{SPH}: 3.0 μg · mL^{-1}

3.4.2. Effect of Ery B concentration

The experiment results indicate that the RRS intensity is maximum when the Ery B concentration is 3.6×10^{-5} mol L^{-1}. If the concentration of Ery B was greater, the Ery B self-aggregation would be reduced, but if the concentration of Ery B was lower than that level, the reaction would be incomplete. Therefore, 3.6×10^{-5} mol L^{-1} was chosen as a suitable Ery B concentration.

3.4.3. Effect of ionic intensity

The effect of ionic strength on the RRS intensity was investigated using a 1.0 mol L^{-1} NaCl solution (Fig. 6). The experimental results show that the RRS intensity decreased dramatically as the ionic strength increased. Therefore, the ion-association reaction should occur in low ionic strength conditions, and salts should be strictly prevented.

3.4.4. Reaction speed and stability

At room temperature, the reaction of the SPH-Ery B system could be completed in 10 min, and the RRS intensity was stable for at least 4 h, but the RRS intensity of the RPH-Ery B system was unstable for the duration of the test.

4. Reaction mechanism and causes of the RRS enhancement

4.1. Formation of an ion-association complex

Using Job's method of continuous variation and the molar ratio method, the composition ratio of SPH with Ery B after the formation of the ion-association complex [24–26] was studied. When the concentration of SPH and Ery B was 8.0×10^{-5} mol L^{-1}, the total volume of SPH and Ery B was 5.0 mL from Job's method and the volume of SPH remained a constant 1.0 mL based on the molar ratio method. Then, the RRS intensity was determined at $\lambda_{em}=\lambda_{ex}=338$ nm, and the result showed that the ratio of SPH to Ery B was 1:1.

To further demonstrate the binding sites and binding mode of SPH with Ery B, the ground-state conformation, total energy and charge distribution of SPH and SPH_2^+ were optimized using the Mo62X/CCPVCTZ level of density functional theory (DFT) [27] and the Conductor-Like Polarisable Continuum Model (CPCM) [28]. Fig. 7 shows the most reactive conformations of SPH and SPH_2^+. Because N and O atoms in SPH have lone pairs of electrons with high charge density, they are easily protonated. In an acidic medium, the protonation of the N atom is more stable and becomes positively charged. The structure of the ion-association complex is shown in Fig. 8, which shows that the intensities of the

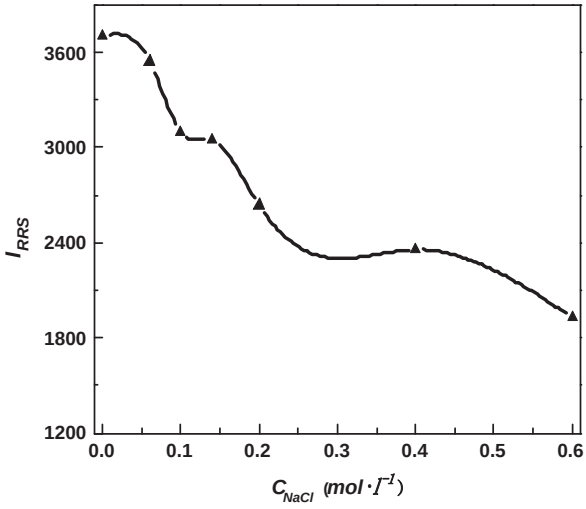

Fig. 6. Effect of ionic strength C_{SPH}: 2.4 μg mL^{-1}; $C_{Ery\ B}$: 3.6×10^{-5} mol L^{-1}; BR, pH=4.6 .

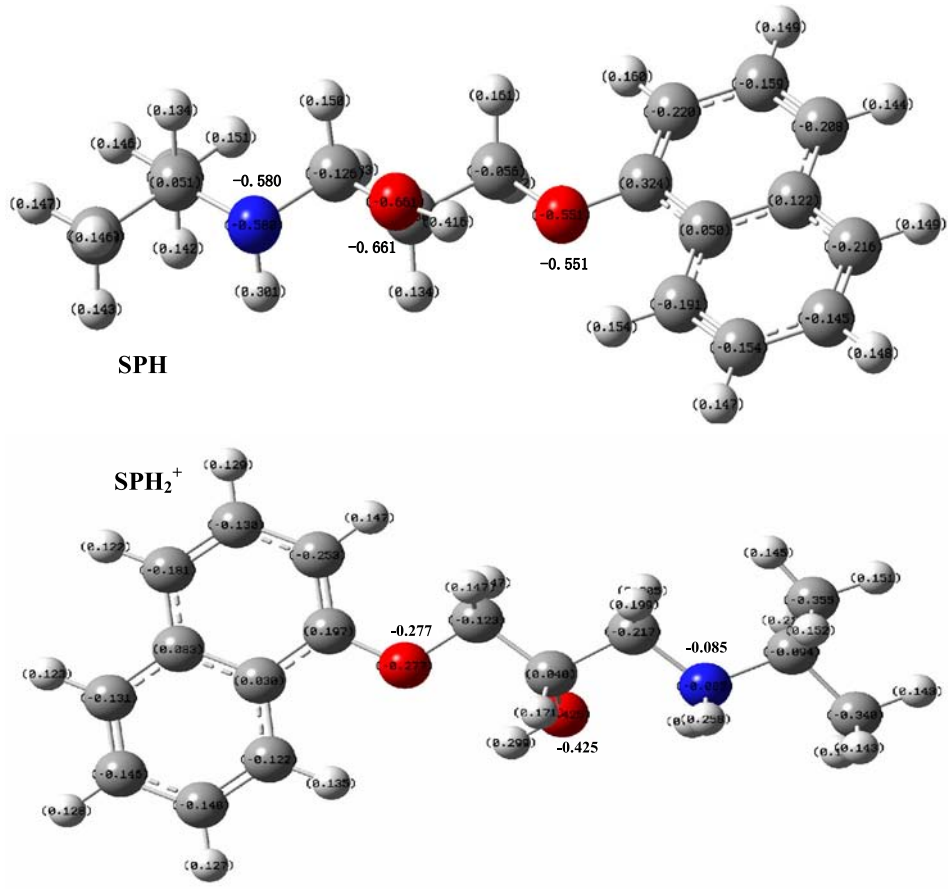

Fig. 7. Optimized conformation and its protonated electronic structures.

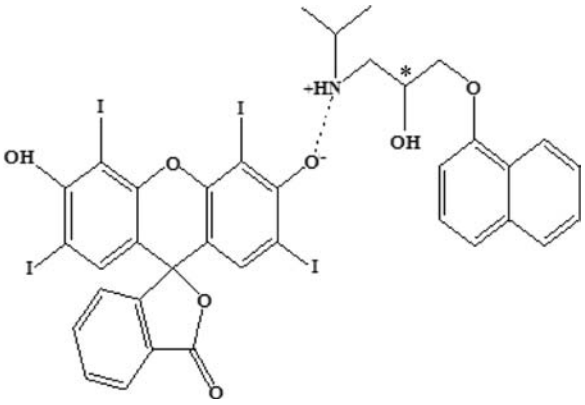

Fig. 8. The structure of binary ion-associate of SPH-Ery B.

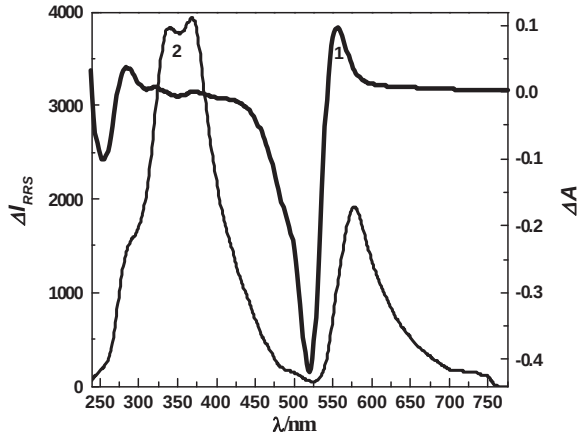

Fig. 9. Comparison of RRS and absorption spectra 1. Absorption spectrum; 2. RRS spectrum; C_{SPH}: 2.4 μg mL^{-1}; $C_{Ery\ B}$: 3.6×10^{-5} mol L^{-1}; BR, pH=4.6.

RRS, FDS and SOS spectra of SPH-Ery B were remarkably enhanced due to steric hindrance, causing them to assume their preferential conformations. In contrast, the RPH-Ery B intensity is very weak and unstable because of its disadvantaged conformation.

4.2. Causes of the RRS enhancement

4.2.1. Effect of the absorption spectra on RRS

When a resonance Raleigh scattering peak is located at or close to the molecular absorption band, the scattering process can absorb the light energy through resonance, resulting in a re-scattering process that produces a significant enhancement in the RRS intensity. Therefore, RRS spectra should be closely related to the absorption spectra [29], which can be observed from a comparison of the RRS and absorption spectra (see Fig. 9); two RRS peaks at 338 nm and 578 nm closely correspond to absorption peaks at 259 nm and 556 nm, respectively. Thus, the RRS intensity was remarkably increased. Therefore, the resonance Raleigh scattering effect has become a considerable force for scattering enhancement.

4.2.2. Enlargement of the molecular volume

According to the Raleigh scattering formula, an increase in the molecular scattering volume is beneficial to the RRS intensity. If the molecular volume is not easy to calculate, it can be substituted by the molecular weight, namely $I=KCMI_0$ [30], where I is the RRS intensity, I_0 the incident intensity, C the solution concentration, K a coefficient and M the molecular weight. When other factors are

constant, the RRS intensity is directly proportional to the molecular weight of the particle. The increase in molecular weight from 296.8 (SPH_2^+) to 1131.7 (SPH-Ery B) before and after the reaction increases the RRS intensity.

4.2.3. Formation of a hydrophobic interface

Before the reaction, the drug and Ery B existed as protonated cations and anions, respectively. Because they are water-soluble ions, they can easily form hydrates in water with low RRS intensities. When the drug and Ery B react with each other to form a neutralized ion-association complex, a hydrophobic liquid-solid interface appears due to the presence of a hydrophobic aryl framework in the binary complex. The formation of the hydrophobic interface increases the RRS signal [31].

4.2.4. Effect of molecular planarity and rigidity

After the formation of the complex, the bond between the positive and negative charges and the rotations of aryl group were restricted due to the increased molecular volume, strengthening the molecular planarity and rigidity, which enhanced the scattering intensity [32].

Table 1
Related parameters for the calibration graphs and the detection limits.

Method	Linear regression equation ($\mu g \cdot mL^{-1}$)	Linear range ($\mu g \cdot mL^{-1}$)	Correlation coefficient (r)	Detection limit (3σ, $ng \cdot mL^{-1}$)	RSD (%)
RRS	$\Delta I = 2362.2 + 610.75c$	0.068 ~ 4.0	0.9998	20.6	2.7
SOS	$\Delta I = 41.20 + 17.86c$	0.173 ~ 4.0	0.9995	52.4	3.1
FDS	$\Delta I = 27.64 + 16.77c$	0.244 ~ 4.0	0.9951	73.9	3.3

To calculate RSD by 7 times parallel determination of SPH 1.0 $\mu g\ mL^{-1}$.

Table 2
Effects of coexisting substances (SPH was 2.0 $\mu g\ mL^{-1}$).

Coexisting substance	Times	Relative error (%)	Coexisting substance	Times	Relative error (%)
NaCl	105.2	+4.3	L-Aspartic acid	18	+2.4
K_2CO_3	110	+2.7	Glycine	30	+2.5
$CaCl_2$	40	+0.2	L-phenylalanine	40	+2.3
$MgCl_2$	50	+1.4	L-Histidine	15	+3.5
$CuCl_2$	15	-0.2	L-Cysteine	50	+4.3
$FeCl_3$	20	-0.5	β-cyclodextrin	30	+1.6
NH_4NO_3	50	+3.0	Glucose	20	+1.4
$MnSO_4$	15	-1.5	Fructose	15	+1.3
$ZnSO_4$	18	+4.8	Barley-sugar	15	+4.0
$Al_2(SO_4)_3$	16	-1.0	Starch	40	+4.3
HSA	10	-4.7	Cellulase	25	+2.7
BSA	20	+3.6	Vitamin C	16	+2.3
D-Tryptophan	60	-3.1	Uric acid	80	-1.1
D-Tyrosine	10	-2.4	Urea	50	-0.9

5. Selectivity, sensitivity and analytical application

5.1. Sensitivity

Under optimum reaction conditions, SPH at different concentrations reacted with Ery B to form ion-association complexes, and the RRS, SOS and FDS spectral intensities were measured at their respective maximum wavelengths. Calibration graphs of ΔI_{RRS}, ΔI_{SOS} and ΔI_{FDS} versus the SPH concentration were constructed. The regression equation, linear range, correlation coefficient (r) and limit of detection and relative standard deviation are listed in Table 1. It can be observed from Table 1 that the RRS method has the highest sensitivity; therefore, the RRS and NRLS methods can be applied to the trace determination of SPH.

5.2. Selectivity

Using the RRS method, the effects of common metal ions, common inorganic anions, proteins, amino acids and sugars on the determination of SPH were investigated, and the results are shown in Table 2. When the SPH concentration was 2.0 $g \cdot mL^{-1}$ and the relative standard deviation was within $\pm 5\%$, large amounts of the common metal ions Ca^{2+} and Na^+, the inorganic anions Cl^- and NO_3^-, urea, glucose, and a large number of amino acids had minimal impacts on the determination of SPH, but the amounts of human serum albumin and bovine serum albumin that can be tolerated are small. If the samples contained these proteins, protein precipitant agents, such as trichloroacetic acid and acetonitrile, should be added to remove them first. Therefore, the method has good selectivity and can be applied to real samples.

5.3. Analytical application

5.3.1. Determination of SPH in human urine samples

Fresh urine samples (healthy human) were centrifuged at 6000 rpm for 20 min. Then, 1.0 mL of the supernatant fluid was pipetted and diluted to 10.0 mL. Next, 3 aliquots of 1.0 mL of this solution were added to a 10.0 mL volumetric flask, and the concentration of SPH was determined. The recoveries and relative standard deviations (R.S.D.) were tested using the standard addition method and five parallel determination results listed in Table 3.

5.3.2. Determination of SPH in human serum samples

Fresh serum samples (healthy human) were treated with suitable amounts of trichloroacetic acid and centrifuged for 5 min at 6000 rpm to remove proteins. Then, 1.0-mL aliquots of the supernatant fluid were diluted to 50.0 mL, and three aliquots of 1.0 mL of this solution were pipetted into a 10.0-mL volumetric flask. The SPH was then determined. The R.S.D. and recovery were examined using the standard addition method and five parallel determination results. Similarly, the method had been validated by comparing with official approaches (Spectrophotometry), these results all are listed in Table 3.

Table 3
Results for the determination of trace SPH in serum and urine samples.

Sample	Found ($\mu g \cdot mL^{-1}$)	Added ($\mu g \cdot mL^{-1}$)	This method			Spectrophotometry		
			Found ($\mu g \cdot mL^{-1}$, $n=5$)	RSD (%)	Recovery (%)	Found ($\mu g \cdot mL^{-1}$, $n=5$)	RSD (%)	Recovery (%)
Serum 1	ND[a]	0.8	0.8100 ± 0.025	3.1	101.2	0.798 ± 0.035	4.4	99.8
Serum 2	ND[a]	0.9	0.9135 ± 0.020	2.2	101.5	0.896 ± 0.033	3.7	99.5
Serum 3	ND[a]	1.0	1.0234 ± 0.035	3.4	102.3	0.989 ± 0.028	2.8	98.9
Urine 1	ND[a]	1.0	1.0012 ± 0.031	3.1	100.1	0.991 ± 0.032	3.2	99.1
Urine 2	ND[a]	1.5	1.5228 ± 0.045	3.0	101.5	1.481 ± 0.061	4.1	98.7
Urine 3	ND[a]	2.0	2.0518 ± 0.050	2.4	102.6	1.992 ± 0.059	3.0	99.6

[a] ND: Not detected by this method.

6. Conclusion

In a weakly acidic medium, SPH and RPH can react with Ery B through electrostatic attraction and hydrophobic forces to form 1:1 ion-association complexes. Both SPH and RPH can alter the absorption spectra of erythrosine B. The SPH-Ery B system resulted in a remarkable enhancement of RRS, FDS and SOS. However, a similar phenomenon was not observed in the RPH-Ery B system. Based on this result, a novel spectral method with high sensitivity, good selectivity, rapidity and simplicity for the determination of trace SPH was proposed and successfully applied to the determination of SPH in serum and urine samples. This result may aid in the chiral recognition of enantiomer drugs. Furthermore, it is anticipated that this new information will provide a more convenient and simpler method to analyze both enantiomers of propranolol hydrochloride simultaneously.

Acknowledgments

This work was financially supported by the National Science Foundation of China (NO.21175015), and all authors here express their deep gratitude.

References

[1] M. Fillet, I. Bechet, P. Chiap, P. Hubert, J. Chromatogr. A 717 (1995) 203–209.
[2] H. Kim, K. Jeong, S. Lee, S. Jung, B. Kor, Chem. Soc 24 (2003) 95–98.
[3] A. SK, R. Mohan Rao Ch, D. Rao G, A. L. Rao, Ph. Tech. Med 1 (2012) 53–58.
[4] J.R. Zhang, H. Pang, Chin. J. Pharmaceutical 27 (1996) 516–518 (In Chinese).
[5] L.P. Shen, S.H. Xing, Chin. J. Pharmaceutical Biomed 12 (2003) 34–35 (In Chinese).
[6] H.Y. Ma, J.J. Luo, M. Yang, J.W. Xin, Ptca (Part B: Chem. Anal.) 46 (2012) 674–677.
[7] W. Huang, F. Wang, X.J. Liu, F.L. Cl, Cent. South Pharm. 5 (2007) 40–42.
[8] C.Y. Ma, Chin. Pharm 8 (2005) 637–638 (In Chinese).
[9] Z. Rao, Q. Wu, G. Xie, H. Xu, X. Zhang, Chin. J. Anal. Chem. 32 (2004) 1660–1662 (In Chinese).
[10] L. Kong, Z.F. Liu, X.L. Hu, S.P. Liu, Microchim. Acta 173 (2011) 207–213.
[11] X. Long, C. Zhang, J. Cheng, S. Bi, Spectrochim. Acta A 69 (2008) 71–77.
[12] H.Q. Luo, N.B. Li, S.P. Liu, Biosens. Bioelectron. 21 (2006) 1186–1194.
[13] X.L. Hao, N.B. Li, H.Q. Luo, Spectrochim. Acta A 71 (2009) 1673–1677.
[14] T.S. Li, S.P. Liu, Z.F. Liu, X.L. Hu, Arch. Pharm. 338 (2005) 427–432.
[15] S. Liu, Z.Y. Zhang, X.L. Hu, Z.F. Liu, F. Wang, Chin. J. Analytical Chem. 33 (2005) 989–992 (In Chinese).
[16] S.P. Liu, Z.F. Liu, H.Q. Luo, Analytical Chim. Acta 407 (2000) 255–260.
[17] X.F. Long, S.P. Bi, H.Y. Ni, X.C. Tao, N. Gan, Analytical Chim. Acta 501 (2004) 89–97.
[18] L. Kong, S.P. Liu, J. Int., Environ. Analytical 93 (2013) 23–34 (Chem).
[19] P. Wang, J.X. Dong, N.B. Li, H.Q. Luo, Spectrochim. Acta A 103 (2013) 38–44.
[20] S.P. Liu, F. Wang, Z.F. Liu, X.L. Hu, A.E. Yi, H. Duan, Analytical Chim. Acta 601 (2007) 101–107.
[21] P.L. Chen, X.L. Hu, S.P. Liu, Z.F. Liu, Y.Q. Song, Spectrochim. Acta A 77 (2010) 207.
[22] J. Liu, Z.F. Liu, X.L. Hu, L. Kong, S.P. Liu, J. Pharmaceutical Biomed 43 (2007) 1452–1459.
[23] M.Y. Qin, S.P. Liu, Z.F. Liu, X.L. Hu, Spectrochim. Acta A 71 (2009) 2063–2068.
[24] D.P. Xu, S.P. Liu, Z.F. Liu, X.L. Hu, Analytical Chim. Acta 588 (2007) 10–15.
[25] F.L. Tian, J.D. Yang, W. Huang, S. Zhou, G.Y. Yao, Spectrochim. Acta A 116 (2013) 57–64.
[26] Y.Q. Song, S.P. Liu, Z.F. Liu, X.L. Hu, Spectrochim. Acta A 78 (2011) 148–152.
[27] M. Orio, D.A. Pantazis, F. Neese, Photosynthesis Res. 102 (2009) 443–453.
[28] Y Takano, K.N. Houk, J. Chem. Theory Computation 1 (2005) 70–77.
[29] J. Anglister, I.Z. Steinberg, J. Chem. Phys. 78 (1983) 5358–5368.
[30] Edition of Editorial Board of Chinese Macropaedia, Chinese Macropaedia Biology (II), Chinese Macropaedia Press, Beijing, 1991, p. 1374 (In Chinese).
[31] S.P. Liu, L. Kong, Analytical Sci. 19 (2003) 1055–1060.
[32] S.P. Liu, L. Fan, X.L. Hu, Z.F. Liu, S. Li, Analytical Sci. 22 (2006) 819–823.